

INFLUENCE OF Na AND Cr SUBSTITUTIONS ON ELECTRONIC PHASE DIAGRAM OF $\text{La}_{0.54}\text{Ho}_{0.11}\text{Ca}_{1-x}\text{Na}_x\text{Mn}_{1-y}\text{Cr}_y\text{O}_3$ MANGANITES

M-L. CRAUS^{1,2}, N. CORNEI³, M. LOZOVAN¹, C. MITA³ and V. DOBREA¹

¹NIRD for Technical Physics, 47 Mangeron B-d., 700050, Iasi, Romania, E-mail: craus@phys-iasi.ro

²LNF – JINR, Dubna, Joliot-Curie 6, 141980 Dubna, Mosk. obl., Russia,

³Chemistry Department of “Al. I. Cuza” University, B-d Carol I, Nr.11, 700506, Iasi, Romania

(Received September 15, 2009)

Abstract. We have synthesized by sol-gel method $\text{La}_{0.54}\text{Ho}_{0.11}\text{Ca}_{1-x}\text{Na}_x\text{Mn}_{1-y}\text{Cr}_y\text{O}_3$ magnetoresistive bulk manganites. The samples contain only a perovskite phase. The substitution of Mn with Cr led to a strengthening of the metallic ferromagnetic phase. An increase of Curie temperature with Cr concentration was observed, for $y < 0.2$.

Key words: manganites, electronic phase diagram, magnetic and crystalline structure, transport phenomena.

1. INTRODUCTION

The $\text{La}_{1-x}\text{Ca}_x\text{MnO}_3$ perovskites (ABO_3) exhibit a strong interplay between the charge, lattice and spin degrees of freedom, being characterized by a transition from paramagnetic insulating (PI) to ferromagnetic metallic (FM) for $x \in (0.2 \div 0.5)$ [1, 2]. The balance between the two phases (PI and FM), with different electronic properties, can be readily influenced by varying physical parameters such as an applied magnetic field, hydrostatic pressure, chemical pressure etc [3, 4]. The nature of magnetic ordering in the entire compositional range depends on the relative concentrations of Mn^{3+} and Mn^{4+} , respectively, structural properties, *via* Mn–O–Mn angles and Mn–O distances. In order to understand the mechanisms involved in the double exchange (DE) interactions, many works have been done then through substitution of the A perovskite-site [4, 5]. This strongly depends on the geometrical features of the perovskite structure, the observed decrease of metal-insulator transition temperature (T_{IM}) with the reduction of average radius of A places being explained by the narrowing of the bandwidth due to a bending of the Mn–O–Mn bond angle. On other hand, the change of the alkaline earth cations on

A places can significantly modify the MR due to the influence on the double-exchange (DE) interaction due to the distortion induced in the $\text{Mn}^{3+}-\text{O}^{2-}-\text{Mn}^{4+}$ network, eventually by the magnetic coupling between the doping and Mn ions [5, 6]. Local distortions of the MnO_6 octahedra determine the charge transport behavior and complex magnetic and crystalline structures. The substitution of Mn with other transition cation destroys the DE interaction, by lowering the Curie temperature and enhancing the magnetoresistance; some authors obtained a large magnetoresistance by substituted Mn with $M = \text{Cr}, \text{Fe}, \text{Ni}$ or Cu in $\text{La}_{0.7}\text{Sr}_{0.3}\text{Mn}_{0.9}\text{M}_{0.1}\text{O}_3$ [5]. The substitution of Mn with Cr leads, on other hand, to the appearance of the phase separation (PS) in Cr-doped manganites $R_{1/2}\text{Ca}_{1/2}(\text{Mn}, \text{Cr})\text{O}_3$ ($R = \text{La}, \text{Nd}, \text{Sm},$ and Eu) [7].

Our purpose is to obtain the electronic phase diagram and to investigate its modifications in $\text{La}_{0.54}\text{Ho}_{0.11}\text{Ca}_{1-x}\text{Na}_x\text{Mn}_{1-y}\text{Cr}_y\text{O}_3$ manganites.

2. EXPERIMENTAL DETAILS

The samples with the chemical composition $\text{La}_{0.54}\text{Ho}_{0.11}\text{Ca}_{1-x}\text{Na}_x\text{Mn}_{0.95}\text{Cr}_{0.05}\text{O}_3$ ($x = 0.05, 0.1$) and $\text{La}_{0.54}\text{Ho}_{0.11}\text{Ca}_{0.35}\text{Mn}_{1-y}\text{Cr}_y\text{O}_{3-\delta}$ ($y = 0.05, 0.10, 0.15$ and 0.20) were prepared by means of sol-gel method, using as precursors rare earth oxides ($\text{La}_2\text{O}_3, \text{Nd}_2\text{O}_3$ and Ho_2O_3) (purity: 99.99%), the calcium carbonate (CaCO_3), sodium nitrate (NaNO_3) and the Mn and Cr acetates (purity: 99.00%). The details of the preparation were already communicated [8, 9]. The resulted powders were ground and pressed into pellets and presintered at 800°C for 17 hours in air. The presintered samples were again ground and finally sintered at 1200°C for 10 hours in air atmosphere. Phase composition, structure, lattice constants and volume of the unit cell were determined by X-ray analysis using a HUBER – Guinier Camera 670 diffractometer with a $\text{CuK}\alpha_1$ radiation. The lattice constants, positions of cations and anions in unit cell, BO distances, BOB bond angles, average size of mosaic blocks and microstrains being determinate by using Fullprof or PowderCell code. The space group was selected by means of the Ceckcell program. Specific magnetization with temperature and Curie temperature were determined by using a VMS type magnetometer, working at $H = 1$ T, between 77 and 400 K. The Curie temperature (T_C) was determined as corresponding to the point where first derivative vs. temperature (T) has a minimum [10]. The variation of resistance with temperature and magnetic field was performed with a close cycle refrigerator, working between 7 and 350 K, at $H_{\text{max}} = 1$ T. The transition temperature from metallic to insulator (T_M) state is marked by the change of resistivity derivative with temperature (resistance) from $d\rho/dT > 0$ to $d\rho/dT < 0$. In agreement with literature data, we consider the transition temperature as the temperature corresponding maximum of the resistivity vs. T , at $H = 0$ [11].

3. RESULTS AND DISCUSSIONS

The analysis of the X-ray diffraction pattern showed that all the samples contain only an orthorhombic phase with perovskite structure, Pnma type structure (Figs. 1, 2). The substitution of Ca with Na leads to an increase of the unit cell volume and lattice constants, of the Mn-O (B-O) distances, of the deformation of the unit cell and of the microstrains level (Table 1), in agreement with the Shannon's ionic radii of Ca^{2+} and Na^+ ($r_{\text{Ca}^{2+}} = 1.18 \text{ \AA}$, $r_{\text{Na}^+} = 1.24 \text{ \AA}$; for both CN = 9). For $\text{La}_{0.54}\text{Ho}_{0.11}\text{Ca}_{0.35-x}\text{Na}_x\text{Mn}_{0.95}\text{Cr}_{0.05}\text{O}_3$ manganites we observed an increase of the lattice constants, unit cell volume and Mn-O (B-O) distances, as comparing with $\text{La}_{0.54}\text{Ho}_{0.11}\text{Ca}_{0.35}\text{Mn}_{1-y}\text{Cr}_y\text{O}_3$ manganites (x , respectively, y , s . Tabs. 1, 2).

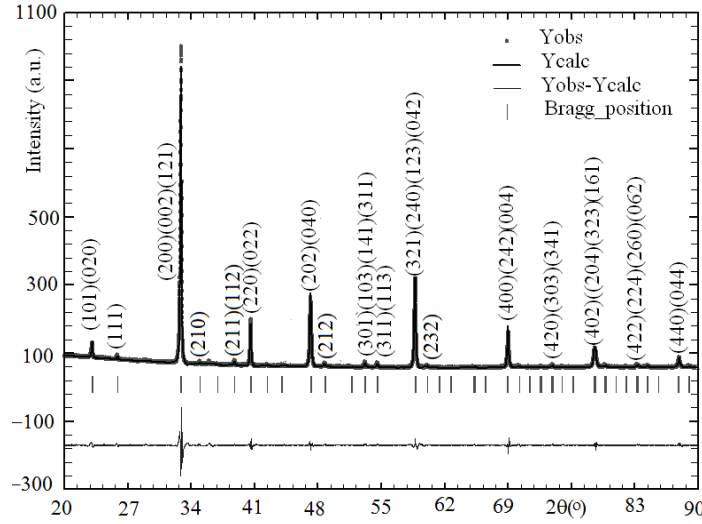
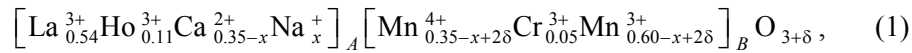


Fig. 1 – The calculated and observed diffractograms of $\text{La}_{0.54}\text{Ho}_{0.11}\text{Ca}_{0.30}\text{Na}_{0.05}\text{Mn}_{0.95}\text{Cr}_{0.05}\text{O}_3$; bottom part: the difference between calculated and observed diffractograms (Fullprof method).

The cation distribution of doped with Na manganite is given by:



where δ is the supplemental oxygen.

Tolerance factor is given by formula:

$$t = \frac{r_A}{\sqrt{2}r_B} = \frac{0.54r_{\text{La}^{3+}} + 0.11r_{\text{Ho}^{3+}} + 0.35r_{\text{Ca}^{2+}} + x(r_{\text{Na}^+} - r_{\text{Ca}^{2+}}) + r_{\text{O}^{2-}}}{\sqrt{2}(0.35r_{\text{Mn}^{4+}} + 0.60r_{\text{Mn}^{3+}} + 0.05r_{\text{Cr}^{3+}} + (x - 2\delta)(r_{\text{Mn}^{3+}} - r_{\text{Mn}^{4+}}) + r_{\text{O}^{2-}})}, \quad (2)$$

where $\langle r_A \rangle$ and $\langle r_B \rangle$ are the average radii of A and, respectively, B places.

On Eq. (2) the calculated $d_{\text{Mn-O}}$ distances and unit cell volumes for doped with Na manganites should increase, with the increase of Na concentration, in agreement with our result (Table 2). The oxygen concentration in the samples, if varies, shows a small influence on average radius of B places. The tolerance factor increases with oxygen concentration and decrease with Na concentration (Eq. 2).

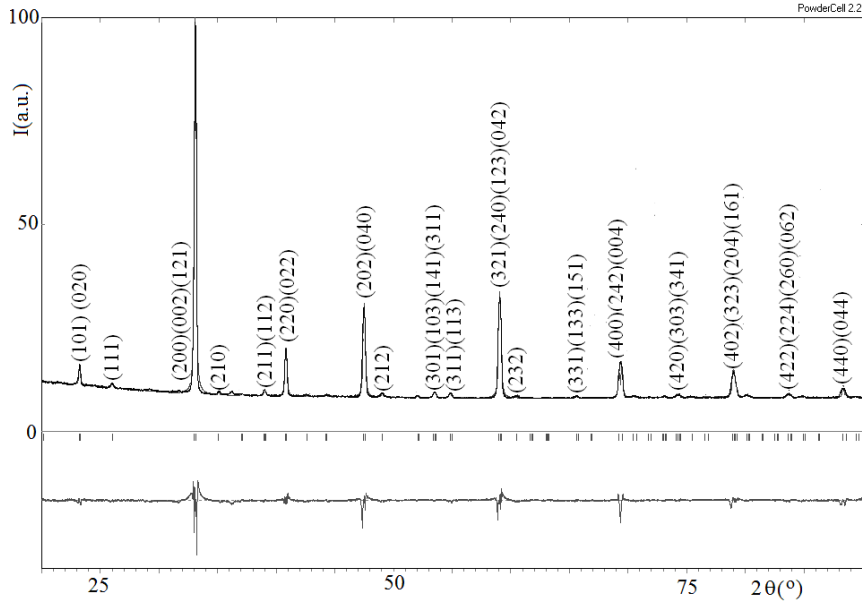


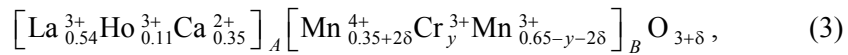
Fig. 2 – The calculated and observed diffractograms of $\text{La}_{0.54}\text{Ho}_{0.11}\text{Ca}_{0.35}\text{Mn}_{0.95}\text{Cr}_{0.05}\text{O}_3$ manganite; bottom part: difference between calculated and observed diffractograms (PowderCell method).

Table 1

The variation of the lattice constants (a , b , c), unit cell volume (V), average size of crystalline blocks (D) and microstrains (ϵ) for $\text{La}_{0.54}\text{Ho}_{0.11}\text{Ca}_{0.35-x}\text{Na}_x\text{Mn}_{0.95}\text{Cr}_{0.05}\text{O}_3$ and $\text{La}_{0.54}\text{Ho}_{0.11}\text{Ca}_{0.35}\text{Mn}_{1-y}\text{Cr}_y\text{O}_3$ manganites

		$a(\text{\AA})$	$b(\text{\AA})$	$c(\text{\AA})$	$V(\text{\AA}^3)$	$D(\text{\AA})$	ϵ
x	0.05	5.4390	7.7041	5.4351	227.75	706	0.00022
	0.10	5.4455	7.6893	5.4481	228.12	624	0.00042
y	0.05	5.4243	7.6357	5.4032	223.79	545	0.00056
	0.10	5.3928	7.6153	5.3635	220.27	1260	0.00094
	0.15	5.3808	7.6082	5.3601	219.43	1123	0.00049
	0.20	5.3817	7.6084	5.3500	219.06	994	0.00046

For Cr doped manganites the cation distribution is given by:



while the tolerance factor will be given by:

$$t = \frac{0.54r_{\text{La}^{3+}} + 0.11r_{\text{Ho}^{3+}} + 0.35r_{\text{Ca}^{2+}} + r_{\text{O}^{2-}}}{\sqrt{2}(0.35r_{\text{Mn}^{4+}} + 0.65r_{\text{Mn}^{3+}} - y(r_{\text{Mn}^{3+}} - r_{\text{Cr}^{4+}}) - 2\delta(r_{\text{Mn}^{3+}} - r_{\text{Mn}^{4+}}) + r_{\text{O}^{2-}})}. \quad (4)$$

The average radius of B places/average d_{BO} distances decrease, while tolerance factor increases with the increase of the Cr and oxygen concentrations (Eq. 3). The observed variation of B/Mn-O distances in Cr substituted manganites can be explained by a superposition of two effects: 1) the increase of the Cr concentration and 2) the decrease of O concentration (Eq. 4 and Table 2).

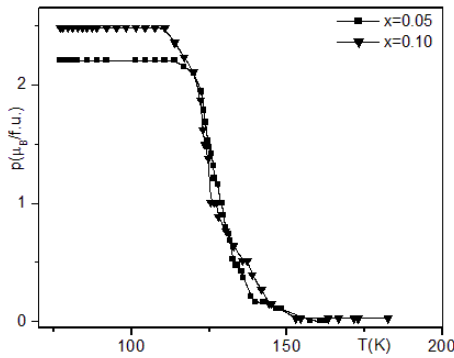


Fig. 3 – The variation of molar magnetization with temperature and Na concentration for $\text{La}_{0.54}\text{Ho}_{0.11}\text{Ca}_{0.35-x}\text{Na}_x\text{Mn}_{0.95}\text{Cr}_{0.05}\text{O}_3$ manganites.

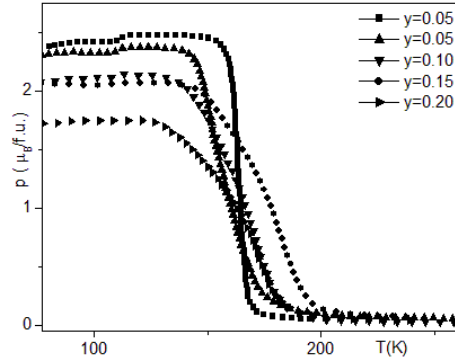


Fig. 4 – The variation of molar magnetization with temperature and Cr concentration for $\text{La}_{0.54}\text{Ho}_{0.11}\text{Ca}_{0.35}\text{Mn}_{1-y}\text{Cr}_y\text{O}_3$ manganites.

Calculated values of magnetic molecular moments, considering only the contribution of all magnetic moments of Mn cations vary between 3.45 and 2.85 $\mu_{\text{B}}/\text{f.u.}$, when the Mn is substituted with Cr metallic cation in stoichiometric manganites. The observed values are much smaller and can be associated with a magnetic matrix in which there are nonmagnetic clusters. The volume of magnetic matrix diminishes when the Na concentration increases. Concerning the magnetic properties, we observed that the Curie temperature are smaller than thus corresponding to undoped with Ho, Na or Cr manganites, with the same Ca concentration [2].

The decrease of the Curie temperature, when Ho substituted La, was expected, because it takes place a decrease of double exchange interactions due to the decrease of the average radius of A places, of the Mn-O-Mn bond angle, implicitly, a smaller superposition of Mn and O orbitals. The substitution of Ca with K, an ion with a radius larger than thus of Ca ($r_{\text{K}^{+}} = 1.55 \text{ \AA}$) led to an increase of the Curie temperature and of the specific magnetization, the latest smaller as

theoretical values [2]. A supplemental decrease of the Curie temperature takes place in the $\text{La}_{0.54}\text{Ho}_{0.11}\text{Ca}_{0.35-x}\text{Na}_x\text{Mn}_{0.95}\text{Cr}_{0.05}\text{O}_3$ manganites, as comparing with the $\text{La}_{0.67}\text{Ca}_{0.33-x}\text{K}_x\text{MnO}_3$ doped with K manganites [2], due to the increase of the Mn-O bonds length and of a small increase of the variance of average radius of A places with Na concentration (Table 2).

Table 2

Variation of the observed values of molar magnetization (p), Curie temperature (T_C), average distance Mn-O ($d_{\text{Mn-O}}$), tolerance factor (t_{obs}), bandwidth (w) and A places radii variance (σ^2) for $\text{La}_{0.54}\text{Ho}_{0.11}\text{Ca}_{0.35-x}\text{Na}_x\text{Mn}_{0.95}\text{Cr}_{0.05}\text{O}_3$ and $\text{La}_{0.54}\text{Ho}_{0.11}\text{Ca}_{0.35}\text{Mn}_{1-y}\text{Cr}_y\text{O}_3$ manganites

		p ($\mu_B/\text{f.u.}$)	T_C (K)	$d_{\text{Mn-O, obs}}$ (Å)	t_{obs}	w^*	σ^{2**}
x	0.05	2.201	128	1.9489	0.932	0.095	0.00205
	0.10	2.478	124	1.9508	0.933	0.095	0.00216
y	0.05	2.370	151	1.9381	0.925	0.097	0.00193
	0.10	2.133	171	1.9261	0.921	0.100	0.00193
	0.15	2.061	182	1.9249	0.903	0.100	0.00193
	0.20	1.748	173	1.9253	0.933	0.100	0.00193

$$*) \ w\alpha \frac{\cos\left[\frac{1}{2}(\pi - \langle \text{MnO Mn} \rangle)\right]}{d_{\text{MnO}}^{3.5}}; \quad **) \ \sigma^2 = \sum C_i r_{iA}^2 - \langle r_A \rangle^2; \quad C_i - \text{concentration of } i \text{ atom on A places}$$

One of the reason of the observed variation of the magnetic moment can be due to the increase of the Mn tetravalent cations concentration (Fig. 3 and Eq. 1), induced by the increase of O concentration. A variation of δ from 0.007 to 0.05 leads to a variation of molar magnetization from 2.201 to 2.478 $\mu_B/\text{f.u.}$, if we consider that the magnetization is due only to the presence of the $\text{Mn}^{3+}\text{-Mn}^{4+}$ pars. In the Cr doped manganites the monotonous decrease of molar magnetization can be attributed to a decrease of $\text{Mn}^{3+}\text{-Mn}^{4+}$ pars concentration, associated with the oxygen concentration decrease with Cr concentration (Eq. 3, Table 2 and Fig. 4).

The substitution of Mn with Cr leads to the suppression of the long range ferromagnetic interactions after the localization of charge carriers [12]. A good correlation was observed between the Curie temperature, on a hand, and average distance B(Mn)-O, on other hand, confirming this scenario (Table 2). The increase of Cr concentration has little influence on the bandwidth (w), but leads to an expected decrease of B-O average bond length, for $x \leq 0.15$ (Table 2).

Taking account the values of molar magnetization, we consider that at temperatures lower as transition temperatures the investigated manganites are formed by a metallic magnetic matrix, in which there are insulator clusters. Both electronic phases have the same crystalline structure.

We suppose that the ferromagnetic regions are formed by $\text{Mn}^{3+}\text{-O-Mn}^{4+}$ bonds, supposition confirmed by the observed values of molar magnetization for $y = 0.05$, in $\text{La}_{0.54}\text{Ho}_{0.11}\text{Ca}_{0.35}\text{Mn}_{1-y}\text{Cr}_y\text{O}_3$ manganites (Table 2). By substituting

stepwise Mn with Cr cations, we observed a diminishes a molecular magnetization (Table 2), which implies a decrease of number of $\text{Mn}^{3+} - \text{O} - \text{Mn}^{4+}$ bonds, characterized by a DE interaction (we supposed that we attained the saturations by applying a magnetic field with intensity about 1 T).

The probability of appearance of a larger number of $\text{Mn}^{4+} - \text{O}^{2-} - \text{Cr}^{3+}$ bonds increases with the increase of Cr concentration in the samples. On the experimental results concerning magnetic molecular moments we concluded that $\text{Mn}^{4+} - \text{O}^{2-} - \text{Cr}^{3+}$ bonds are present and are super-exchange type, its contribution to the magnetic moment of the sample being very small. On other side the double exchange interaction increases with the decrease of Mn-O distance, leading to a corresponding increase of Curie temperature (Table 2).

Table 3

Variation of the transition temperature (T_{MI}), maximum observed resistance at $H = 0$ ($R_{\text{max}, H=0}$) and magnetoresistance (MR_{max}) with Na and Cr concentrations in $\text{La}_{0.54}\text{Ho}_{0.11}\text{Ca}_{0.35-x}\text{Na}_x\text{Mn}_{0.95}\text{Cr}_{0.05}\text{O}_3$ and $\text{La}_{0.54}\text{Ho}_{0.11}\text{Ca}_{0.35}\text{Mn}_{1-y}\text{Cr}_y\text{O}_3$ manganites

		T_{MI} (K)	$R_{\text{max}, H=0}$ (Ω)	MR_{max} (%)
x	0.05	90	1,273	50
	0.10	55	3,325	23
y	0.05	70	270	30
	0.10	55	2,590	37
	0.15	< 7	130,000	38
	0.20	< 7	–	–

The substitutions of Mn with Cr or of Ca with Na lead to a decrease of the transition temperature and to an increase of resistance of the samples. The observed magnetoresistance decreases with Na concentration and increases with Cr concentration in the samples (Table 3 and Figs 5).

The data with magnetoresistance behavior include the samples up to $y = 0.15$. The samples corresponding to $y = 0.20$ have a very large resistance ($> 20 \text{ M}\Omega$) even at relatively high temperature. Increase of resistance at low temperature indicate the presence of a semiconductor (insulator) phase, which increase as concentration with increase of Na or Cr concentration in the manganites.

The increase of the Mn^{4+} concentration contributes to the enhancement of holes in the e_g band, which should leads to a decrease of resistivity of the samples. We have observed an increase of the resistance, respectively, a decrease of the magnetoresistance with the Na concentration (Fig. 5a).

This behaviour is different as comparing with those of $\text{La}_{0.7}\text{Ca}_{0.3-y}\text{K}_y\text{MnO}_3$ manganites [2], probably due to the difference between average radii of A places.

Substitution of Mn with Cr leads to an increase of disorder on the B places lattice. The Cr^{3+} cation is isoelectronic with Mn^{4+} cation ($t_{2g}^3 e_g^0$) and its substitution reduces the number of active Jahn-Teller Mn^{3+} cations. It is suggesting that Cr^{3+} cations are antiferromagnetically coupled with its nearest neighbors (Mn cations), resulting ferromagnetic nanoclusters around each Cr cation.

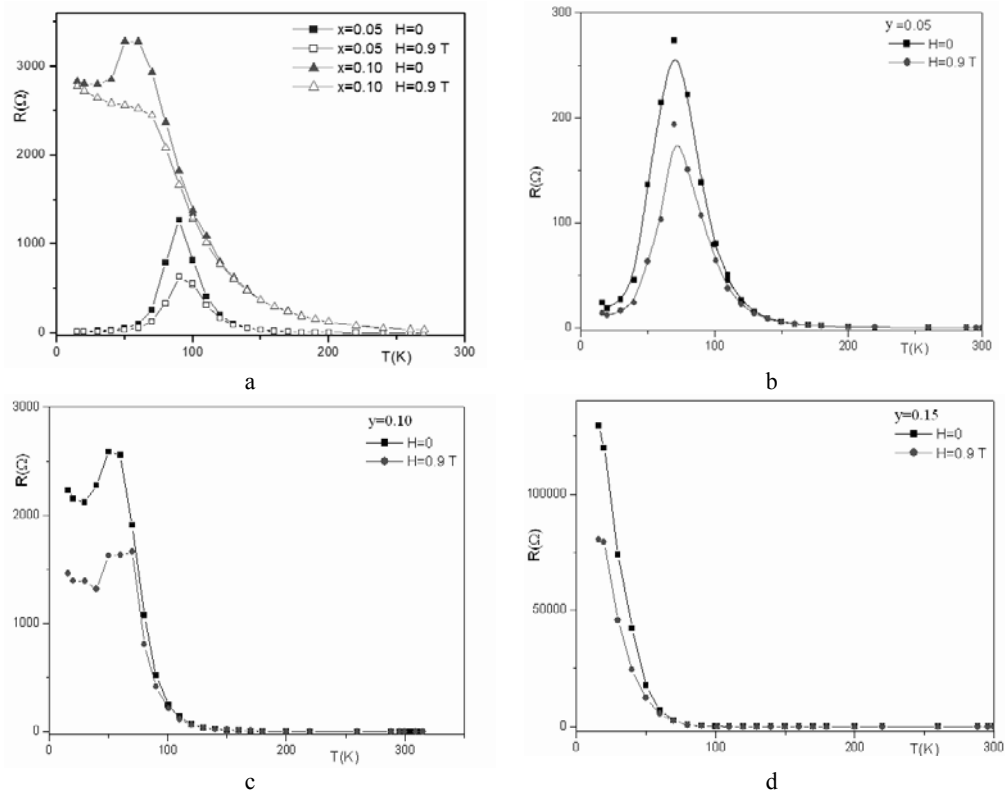


Fig. 5 – The variation of resistance with temperature and intensity of magnetic field for $\text{La}_{0.54}\text{Ho}_{0.11}\text{Ca}_{0.35-x}\text{Na}_x\text{Mn}_{0.95}\text{Cr}_{0.05}\text{O}_3$ (a) and $\text{La}_{0.54}\text{Ho}_{0.11}\text{Ca}_{0.35}\text{Mn}_{1-y}\text{Cr}_y\text{O}_3$ manganites (b, c, d).

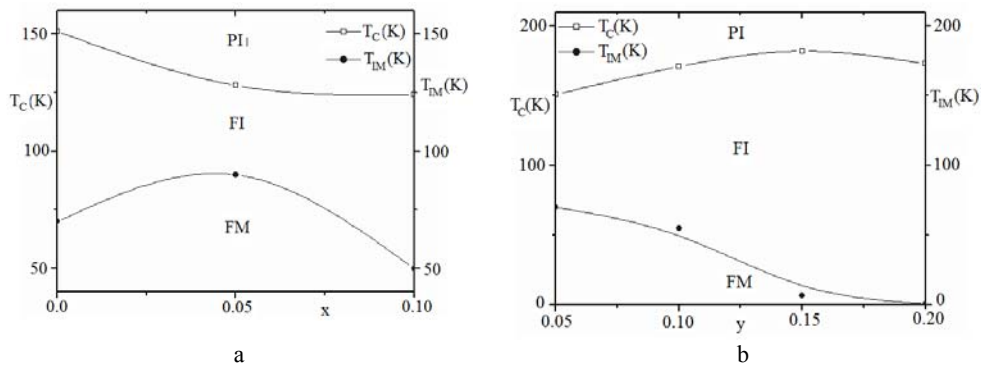


Fig. 6 – The electronic phase diagram of $\text{La}_{0.54}\text{Ho}_{0.11}\text{Ca}_{0.35-x}\text{Na}_x\text{Mn}_{0.95}\text{Cr}_{0.05}\text{O}_3$ (a) and $\text{La}_{0.54}\text{Ho}_{0.11}\text{Ca}_{0.35}\text{Mn}_{1-y}\text{Cr}_y\text{O}_3$ (b) manganites.

It is known that the main obstacle to obtain suitable applications is the fact that the crystalline structure and the microstructure depend on the preparation

methods and treatments. Sol-gel methods produce high quality, homogeneous and fine particle samples. In this context, the method applied to obtain the investigated samples assures the achievement of a single-phase material, with well crystallized grains. However, a concentration of defaults remains after thermal treatment of the samples. We consider that the difference between the Curie and transition temperatures are due to the defaults induced by the presence of the larger/smaller cations than the average size of A and B places in manganites.

Between Curie and transition temperatures of $\text{La}_{0.54}\text{Ho}_{0.11}\text{Ca}_{0.35-x}\text{Na}_x\text{Mn}_{0.95}\text{Cr}_{0.05}\text{O}_3$ and $\text{La}_{0.54}\text{Ho}_{0.11}\text{Ca}_{0.35}\text{Mn}_{1-y}\text{Cr}_y\text{O}_3$ manganites behave as ferromagnetic insulators (semiconductors). It is possible also that the difference between T_C and T_{MI} is appears due to the default regions (especially boundaries layers), which play an important role in variation of (extrinsic) magnetoresistance with temperature. In the boundaries layers the distortions of perovskite lattice are larger as in the crystalline “core”.

The modification of relative position of oxygen and rare earth/alkaline earth ions leads to a decrease of double exchange local interaction, implicitly of the Curie temperature. A monotonous increase of T_C-T_{MI} difference with microstrains level can be observed for $\text{La}_{0.54}\text{Ho}_{0.11}\text{Ca}_{0.35-x}\text{Na}_x\text{Mn}_{0.95}\text{Cr}_{0.05}\text{O}_3$ and $\text{La}_{0.54}\text{Ho}_{0.11}\text{Ca}_{0.35}\text{Mn}_{1-y}\text{Cr}_y\text{O}_3$ manganites (Tables 1 and 2). It means that really exists an influence of defaults concentration on the extrinsic magnetoresistance, implicitly on the observed transition temperature.

Electronic phases diagrams of $\text{La}_{0.54}\text{Ho}_{0.11}\text{Ca}_{0.35}\text{Mn}_{1-y}\text{Cr}_y\text{O}_3$ and $\text{La}_{0.54}\text{Ho}_{0.11}\text{Ca}_{0.35-x}\text{Na}_x\text{Mn}_{0.95}\text{Cr}_{0.05}\text{O}_3$ manganites represent a superposition of intrinsic and extrinsic properties of the manganites: intrinsic properties (as specific/molecular magnetization, Curie temperature) are determined by the crystalline, without defaults, core of the crystallites, while the extrinsic properties correspond to the crystalline shape and the defaults concentration, which appear specially in the boundaries layers of the crystallites. In agreement with the literature [13], the magnetic properties of $\text{La}_{0.67}\text{Ca}_{0.33}\text{MnO}_3$, should depend on the dimension of the crystallites, implicitly by the treatment temperature, due to the boundary layer, which relative volume increases with the decrease of the grain size. Our samples treated at $1,200^\circ\text{C}$ should have a large enough average size, about $1-5\ \mu\text{m}$ (proofed on other manganites), if we take account on the data from Ref. 13, to attain saturation in a relatively small magnetic field. The boundaries layers having, due to the defaults, a very large resistivity have a large influence on the transport mechanism as the crystalline “core”. In these conditions, the transition metal-insulator, characteristic for crystalline “core”, cannot be observed, due to relatively small values of the crystalline “core” resistivity, as compared with the resistivity of the boundaries layers. On other hand, due to its small volume, the boundary layers have a small contribution to the total magnetic moment of the samples. Concerning the observed values of T_C and T_{MI} , its results from difference

between 1) the volume of crystalline “core” and those of boundaries layers of the crystallite, 2) resistivity of the boundaries layers and those of the crystalline “core” and their dependence on the temperature and applied magnetic field.

4. CONCLUSIONS

Two pure row of manganites, $\text{La}_{0.54}\text{Ho}_{0.11}\text{Ca}_{0.35}\text{Mn}_{1-y}\text{Cr}_y\text{O}_3$ and $\text{La}_{0.54}\text{Ho}_{0.11}\text{Ca}_{0.35-x}\text{Na}_x\text{Mn}_{0.95}\text{Cr}_{0.05}\text{O}_3$ were obtained by sol-gel method. For both sets of manganites was observed a large difference between the Curie and transition temperature, attributed to the presence of a large amount of defaults, present in the boundaries layers. The boundary layer with a large amount of defaults and a high resistivity as the “crystalline core” “masks” the transition temperature of the “crystalline core”. The samples can be described as a mixture of a magnetic region, due to the presence of Mn^{3+} -O- Mn^{4+} bonds, characterized by DE interactions. The substitutions of Ca and Mn cations with Na and, respectively, Cr cations in $\text{La}_{0.54}\text{Ho}_{0.11}\text{Ca}_{0.35}\text{Mn}_{1-y}\text{Cr}_y\text{O}_3$ and $\text{La}_{0.54}\text{Ho}_{0.11}\text{Ca}_{0.35-x}\text{Na}_x\text{Mn}_{0.95}\text{Cr}_{0.05}\text{O}_3$ led have opposed influence on the magnetoresistance.

REFERENCES

1. T. Chatterji, D. Andeica, R. Suryanarayana, A. Revcolevschi, *μSR studies of the electron-doped $\text{Ca}_{1-x}\text{Sm}_x\text{MnO}_3$* , Physica B, **374–375**, 59–62 (2006).
2. S. Bhattacharya, S. Pal, R.K. Mukherjee, B.K. Chaudhuri, S. Neeleshwar, Y.Y. Chen, S. Mollah, H.D. Yang, *Development of pulsed magnetic field and study of magnetotransport properties of K-doped $\text{La}_{1-x}\text{Ca}_x\text{MnO}_3$ CMR materials*, J.M.M.M., **269**, 359–371 (2004).
3. S. Ishihara, J. Inoue and S. Maekawa, *Effective Hamiltonian in manganites: Study of the orbital and spin structures*, Phys. Rev., B **55**, 8280–8286 (1997).
4. A. Takahashi and H. Shiba, *Possible Orbital Orderings in a Model of Metallic Double-Exchange Ferromagnets*, J. Phys. Soc. Jpn., **69**, 3328–3333 (2000).
5. X. H. Li, Y. H. Huang, C. H. Yan, Z. M. Wang, C. S. Liao, *Enhanced low field magnetoresistance in Mn substituted nanocrystalline $\text{La}_{0.7}\text{Sr}_{0.3}\text{Mn}_{0.9}\text{M}_{0.1}\text{O}_3$* , J. Phys.: Condens. Matter, **14**, L177–L183 (2002).
6. F. Chen, H. W. Liu, K. F. Wang, H. Yu, S. Dong, X. Y. Chen, X. P. Jiang, Z. F. Ren, J-M Liu, *Synthesis and characterization of $\text{La}_{0.825}\text{Sr}_{0.175}\text{MnO}_3$ nanowires*, J. Phys.: Condens. Matter, **17**, L467–L475 (2005).
7. Y. Morimoto, A. Machida, S. Mori, N. Yamamoto and A. Nakamura, *Electronic phase diagram and phase separation in Cr-doped manganites*, Phys. Rev., B **60**, 9220–9223 (1999).
8. N. Cornei and M.-L. Craus, *Influence of the rare earth cation ($\text{Ln} = \text{La}, \text{Nd}, \text{Sm}$) on the properties of the $\text{Ln}_{0.44}\text{Ho}_{0.11}\text{Sr}_{0.45}\text{MnO}_{3+\delta}$ manganite oxides*, J. of Alloys Comp., **368**, 58–61, (2004).
9. N. Cornei, C. Mita, O. Mentre, F. Abraham, M.-L. Craus, *Synthesis, structural analysis and magnetic properties of Sc-doped $\text{Nd}_{0.8}\text{Sr}_{0.2}\text{Mn}_{1-x}\text{Sc}_x\text{O}_3$ manganites*, J. Opt. and Adv. Mater., **10**, 3300–3304, (2008).
10. S. Rößler, U. K. Rößler, K. Nenkov, D. Eckert, S. M. Yusuf, K. Dörr and K.-H. Müller, *Rounding of a first-order magnetic phase transition in Ga-doped $\text{La}_{0.67}\text{Ca}_{0.33}\text{MnO}_3$* , Phys. Rev., B **70**, 104417 (2004).

11. J. Yang, W. H. Song, Y. Q. Ma, R. L. Zhang, B. C. Zhao, Z. G. Sheng, G. H. Zheng, J. M. Dai and Y. P. Sun, *Structural, magnetic, and transport properties in the Pr-doped manganites $La_{0.9-x}Pr_xTe_{0.1}MnO_3$ ($0.0 \leq x \leq 0.9$)*, Phys. Rev., B **70**, 144421 (2004).
12. C. Castellano, F. Cordero, O. Palumbo, R. Cantelli, A. Martinelli and M. Ferretti, *Local Order and Structure in Mn-Substituted Manganites Studied by EXAFS*, J. Superconductivity: Incorporating Novel Magnetism, **18**, 643–647 (2005).
13. L. E. Hueso, J. Rivas, F. Rivadulla and M. A. Lopez-Quintela, *Tuning of colossal magnetoresistance via grain size change in $La_{0.67}Ca_{0.33}MnO_3$* , J. Appl. Phys., **86**, 3881–3884 (1999).